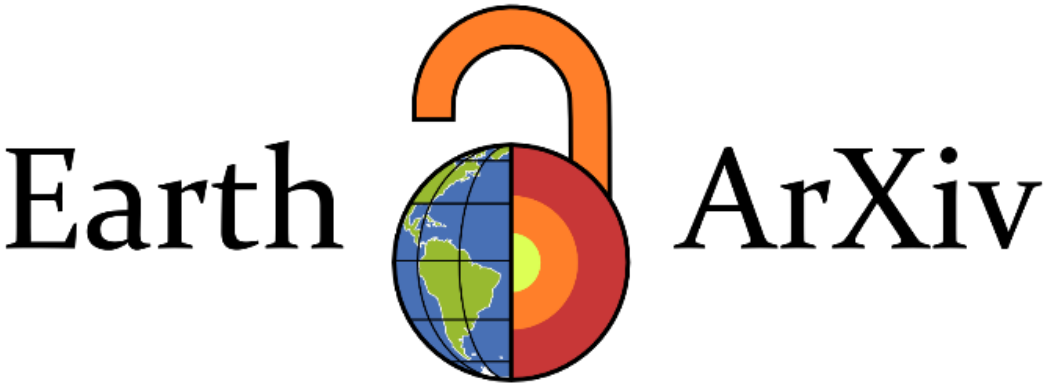

Please send any comments, feedback, or suggestions to benjamin.hatchett@colostate.edu

Highlights

Revisiting Pyroclimographs[⋆]

Benjamin J. Hatchett

- Pyroclimographs use daily satellite fire detections to indicate the seasonality of wildland fire activity.
- Examples across satellite platforms and regions yield considerations when producing pyroclimographs.
- Incorporating additional fire environment data highlights how fire weather deviates from climatology.

Revisiting Pyroclimographs*

Benjamin J. Hatchett[a,#]

[a]*Cooperative Institute for Research in the Atmosphere, Colorado State University, 3925a Laporte Ave, Ft. Collins, 80521, Colorado, United States of America*

Abstract

Wildland fire activity often demonstrates distinct seasonality. Multiple peaks of activity may occur throughout the year with varying magnitudes and durations due to climatologically conducive conditions for wildfire activity or intentional burning. However, anomalous fire environment conditions may favor out-of-season wildfires. Characterization of conditions that increase fire ignition probabilities, extreme fire behavior, and beneficial fire potential enhances our understanding of fire history and past fire behavior while providing insight into how forecast conditions may influence subsequent wildland fires. Here, we apply a commonly-utilized approach to display a region's temperature and precipitation climatology–the climograph–to visually communicate the seasonal cycle, interannual variability, and individual wildland fire events at daily resolution. We use period-of-record satellite observations from the Moderate Resolution Imaging Spectroradiometer and the Visible Infrared Imaging Radiometer Suite. Counts of detections and cumulative fire radiative power provide first-order indicators of elevated or reduced fire activity, either typically (i.e., wildfire season or prescribed burning season) or anomalously (i.e., out-of-season wildfire). Using a case study of Southern California, we show how pyroclimograph results vary as the region of interest shifts and how their interpretation can be complemented with additional fire environment data.

Keywords: climatology, fire weather, remote sensing, visualization, wildland fire

1. Introduction

Climographs display the monthly mean temperature range and total precipitation of a location or region (e.g., Lasantha et al., 2022; Al-Yaari et al.,

*~~This document is the original draft~~. All errors, omissions, and misinterpretations are mine.

#Correspondence to: benjamin.hatchett@colostate.edu

2023). Just as the climate of a region demonstrates a seasonal cycle, many regions also demonstrate a seasonal cycle of fire activity (Swetnam et al., 2011; Al-Yaari et al., 2023; Senande-Rivera et al., 2022). This seasonality results from both the annual march of plant phenology (i.e., a growing season when fuel accumulates and a dormant season when fuel becomes available for combustion) and short- and long-term weather conditions including the onset and termination of seasonal drought, ignition sources from lightning, and otherwise hot, dry, and windy conditions amidst receptive fuelbeds (Dennison and Moritz, 2009).

Linking climatic conditions to the annual cycle of fire activity was first proposed by (Swetnam et al., 2011), who termed the juxtaposition of monthly mean temperature and precipitation with monthly burned area a 'pyroclimograph'. Sablan et al. (2024) developed similar visualizations of monthly fire activity to show the mean, top and bottom 10^{th} percentiles as well as highlight a year of interest (c.f. their Figure 3b). However, wildland fires do not occur on monthly timescales, nor do they always occur during climatologically-mean conditions. This implies a monthly temporal aggregation is potentially less useful to indicate why fire activity occurs either characteristically or anomalously. Further, a monthly aggregation limits our interpretation of how anomalous the environmental conditions were compared to climatology when fire activity increases. Establishing a detailed understanding of the conditions that lead to increased receptiveness of fuels and the potential for extreme fire behavior at ignition- and fuel receptiveness-relevant timescales may support fire management and community adaptation efforts at longer timescales (i.e., annual to decadal) as well as characterizing a region's general fire environment.

The availability of long-term (i.e., decadal) satellite-based fire detections at high resolution in time (i.e., at least daily overflights) and space ($< 1000\ m$), makes it possible to produce climatologies of fire activity at daily resolution. Depending on whether the goal is to support operational fire management or community messaging, long-term planning and adaptation efforts to reduce fire hazard in fire-prone regions, and research activities regarding the fire environment, the region of interest may vary. A region could be jurisdictionally defined, such as a county or National Weather Service County Warning Area. It could also be a physically-defined region such as a watershed, mountain range, or pyrome. Ultimately, the spatial region selected depends on the desired application of the user.

This brief communication provides examples of the different perspectives

offered by a pyroclimograph using three examples from two fire-prone and fire-dependent California landscapes. First, we examine the same region (Colusa County) using different satellite platforms covering different periods-of-record. Second, we show how results vary across the Los Angeles County region using four different geographic boundaries including all or part of the county and surrounding regions. Third, we demonstrate how a more complete pyroclimograph can be produced at the mountain range scale by incorporating additional fire environment data by including weather and fuels information from gridded data products, weather stations, and live fuel moisture observations.

2. Data

We used satellite fire detections from the Moderate Resolution Imaging Spectroradiometer (MODIS) onboard the Aqua (2001–2025) and Terra (2002–2025) spacecrafts and the Visible Infrared Imaging Radiometer Suite (VIIRS; 2012–2025) onboard the Suomi National Polar-Orbiting Partnership (Suomi NPP) spacecraft. Data was acquired from the National Aeronautics and Space Administration's Fire Information for Resource Management System (`https://firms.modaps.eosdis.nasa.gov/`) for the period spanning 1 January 2001 to 31 December 2025. Shapefiles of Colusa and Los Angeles County were acquired from the U.S. Census Bureau (`https://www2.census.gov/geo/tiger/TIGER2025/COUNTY/`). The shapefile for the National Weather Service Los Angeles Weather Forecast Office County Warning Area was acquired from the National Weather Service County Warning Boundary Area Dataset (`https://www.weather.gov/gis/CWABounds`). The boundary of the Los Angeles County Climate Assessment Region, used to support planning and adaptation efforts, was downloaded from the California Open Data Portal (`https://data.ca.gov/dataset/ca-4th-climate-change-assessment-regions`). The Southern California Mountains/Northern Baja pyrome was extracted from (Short et al., 2020). Last, we used the Santa Monica Mountains (a subset of the Transverse Ranges and excluding the Palos Verdes Hills) from the Global Mountain Biodiversity Assessment Mountain Inventory version 2.0 (Snethlage et al., 2022a,b).

To more fully characterize the fire environment, we used period-of-record (January 1995–February 2026) hourly observations of 2 m air temperature, relative humidity and wind speed from the Malibu Hills, California Remote Automatic Weather Station (acquired from the Western Regional Climate

Center at: `https://raws.dri.edu`). Daily, gridded 4 km horizontal resolution estimates of maximum temperature, precipitation, and 100 hour dead fuel moisture spanning 1979–2025 were acquired from the gridMET product (Abatzoglou, 2013). Live fuel moisture observations data for chamise (*Adenostoma fasciculatum*) from six representative sites in the Santa Monica Mountains (Trippet Ranch, Laurel Canyon, Scheuren Road, Clark Motorway, Stunt Road, and Los Robles) with sampling records beginning between 2001–2006, was acquired from the Fuel Moisture Repository Webportal (`https://www.nfmdb.org/`).

3. Methods

All analysis was performed using Matlab (The MathWorks Inc., 2024). Shapefiles from each satellite platform were imported as arrays of fire detection latitude, longitude, fire radiative power (FRP), and time of detection. Desiring maximum detectibility, we did not omit detections based on confidence values. Dates were sorted in descending order of total FRP, and cumulative FRP was calculated to estimate how many days provide 50%, 75% and 90% of the total period-of-record FRP. For individual years, cumulative FRP starting on 1 January are plotted on the upper panel (Figure 1a). For each calendar day across all years, the total number of detections are counted and reported by a bar chart (Figure 1b); specific years of interest can be plotted separately. Cumulative FRP across each calendar day is calculated to show seasonality of fire activity (right hand y-axis of Figure 1b).

For the Santa Monica Mountains example, gridMET-based estimates of daily precipitation were extracted for a box encompassing the region. The daily mean was calculated and aggregated to monthly totals for each year. The top and bottom 5^{th} percentiles and 50^{th} percentile was estimated for each month to demonstrate monthly precipitation variability. The daily mean maximum temperature from gridMET was calculated and the top 5^th and 50^{th} percentile was calculated to provide an estimate of the typical hottest and average maximum temperatures across the year. Similarly, the mean 100 hr dead fuel moisture was calculated and the top and bottom 5^{th} percentiles and 50^{th} percentile was estimated to provide information about the range of moisture conditions of dead fuels in the 100 hr time lag size class (woody material 2.5–7.5 cm in diameter).

A climatology of live fuel moisture was produced by aggregating the six sampling sites and calculating a +/-6 day moving median for each calendar day of the year following (Guirguis et al., 2025). Critically low live fuel moisture values as interpreted by Brown and Shelton (2025) and Dennison and Moritz (2009) provide reference indicators of elevated large fire probability. Fine and dead fuel moisture (FDFM) and probability of ignition (PIG) were calculated hourly at a steep, south aspect level with the fire based on lookup tables (National Wildfire Coordinating Group, 2025). For each calendar day, the lowest 5^{th} percentile FDFM and highest 5^{th} PIG are reported to highlight fuelbed receptiveness to ignition. Last, fire weather hours were estimated using the period-of-record summed daily number of hours meeting the relative humidity ($< 10\%$) and sustained wind speed ($> 6.7\ m\ s^{-1}$ ($> 15\ miles\ hr^{-1}$)) criteria for a Red Flag Warning at the National Weather Service Fire Weather Zones 369 and 37 (California Annual Operating Plan, 2025). For a Red Flag Warning to be issued, these conditions must be sustained for $> 6hr$. This requirement was omitted to yield a more inclusive indicator of when dry and windy conditions climatologically occur.

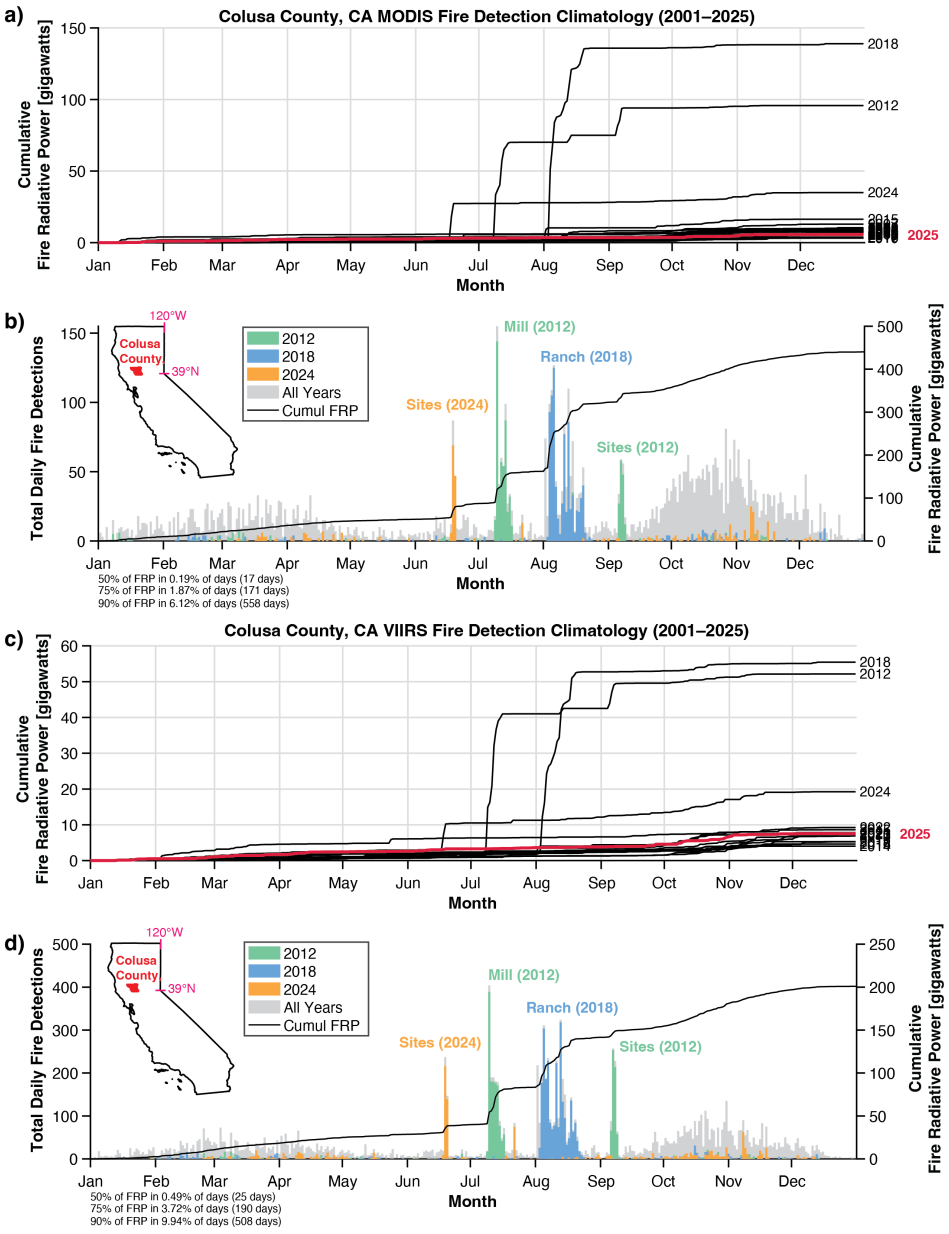

Figure 1: (a) Pyroclimograph showing daily cumulative fire radiative power for each calendar year (2001–2025; black lines; 2025 colored red) using MODIS satellite fire detections for Colusa County, California. (b) Alternative (recommended for singular use) pyroclimograph showing daily (bars; left y-axis) and cumulative (black line; right y-axis) MODIS satellite fire detections for Colusa County, California with notable fires named and colored by year. (c–d) As in (a–b) but produced using the VIIRS instrument onboard the Suomi NPP spacecraft.

4. Results

4.1. Pyroclimographs vary with fire detection input data

Colusa County, CA–an agricultural community–demonstrates three distinct burn seasons as evidenced by shallow increases in annual accumulations of fire radiative power (FRP) during late winter to early spring (mid-January–April), a more rapid increase during the extended summer but dominated by occasional large wildfire incidents (late June–September), and a shift back to shallow but annually consistent increases during fall (October–November; (Figure 1a)). Daily detections (Figure 1b) more clearly indicate the seasonal nature of intentional burning of agricultural lands composed of orchards, vineyards and rice fields) and prescribed burning of wildlands during spring and fall as well as the short duration occasional (e.g., 2012, 2018, and 2024) but higher intensity and larger area (interpreted from the number of detections) of wildfires during the peak warm season. The difference between MODIS (Figure 1a–b) and VIIRS (Figure 1c–d) for Colusa County highlights that VIIRS characteristically yields higher FRP and greater numbers of detections, despite fewer years of observations. In both cases, the trimodal distribution of seasonal fire activity remains evident, but is more pronounced in MODIS due to the relatively higher number of detections during fall and spring owing to the longer period of record. Both satellite products indicate the fractions of total FRP occur over approximately similar periods of time (e.g., 75% of total FRP in 171 days versus 190 days for MODIS and VIIRS, respectively. While the annual cumulative curves allow the comparison of years and events against one another (i.e., to identify early onset of fire activity), for the remainder of the manuscript we focus on the daily bar charts and single annual accumulated FRP (e.g., Figures 1b and 1d).

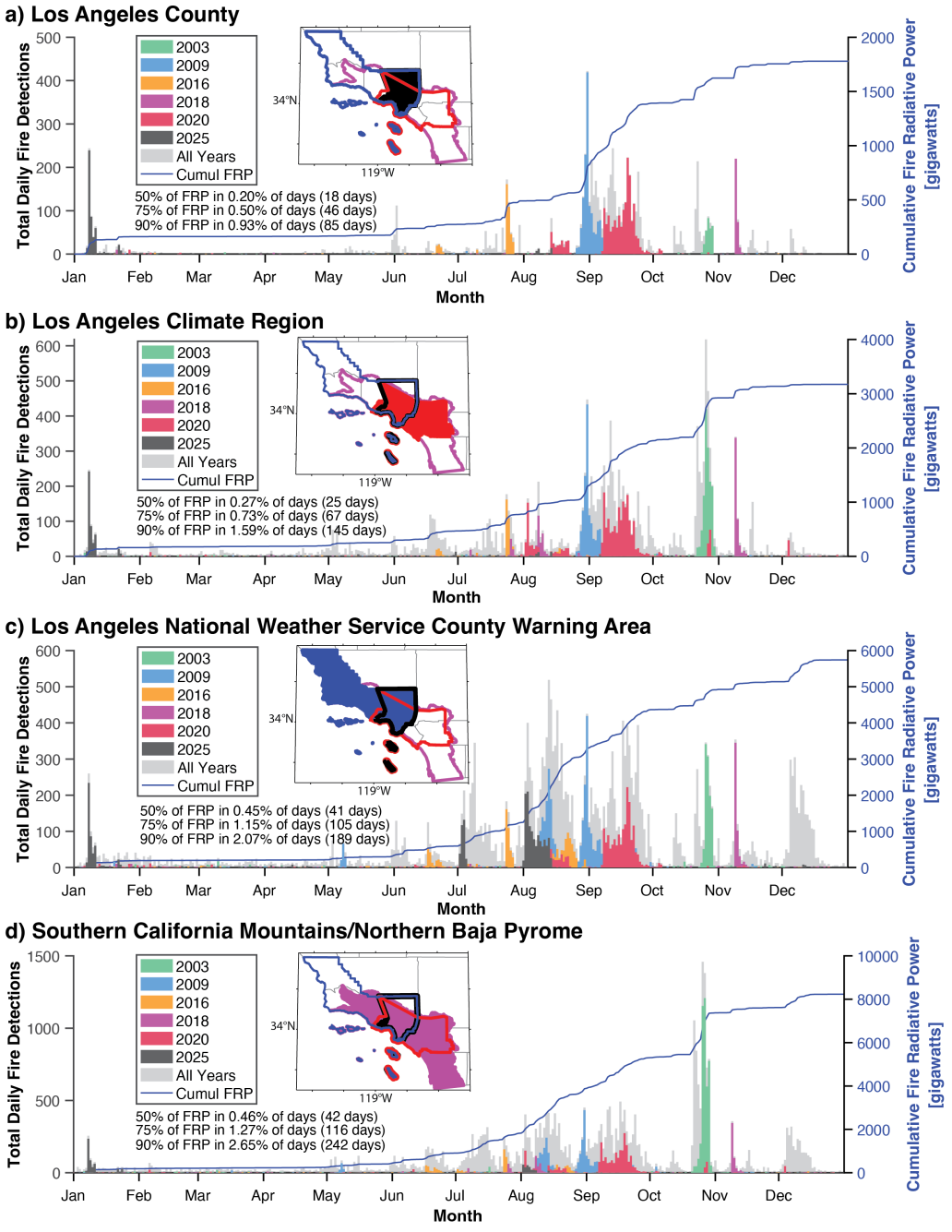

Figure 2: Pyroclimographs for (a) Los Angeles County, California, (b) the Los Angeles California Climate Assessment Region, (c) the Los Angeles National Weather Service County Warning Area, and (d) the Southern California Mountains/Northern Baja Pyrome. Each region is color filled in the associated inset map with other regions outlined.

4.2. Variability across the Los Angeles region

The Los Angeles area of Southern California is a densely populated, fire-prone and fire-dependent but ignition-limited landscape with extraordinary exposure of values-at-risk to wildland fire. The typical Los Angeles County fire season occurs between June and mid-November but centered between August–September (Figure 2a). In the satellite record, the anomalous nature of the January 2025 Los Angeles Fire Disaster is apparent. The Los Angeles Climate Region (Figure 2b) truncates Los Angeles County along the crest of the Transverse and Peninsular Ranges and includes Orange and parts of Riverside and San Bernardino counties. Including additional fire-prone mountain ecosystems, as well as additional populated areas (i.e., ignition sources) extends the periods of peak fire activity earlier into May and includes several additional large fire events in October (2003) and November (2018).

The Los Angeles National Weather Service County Warning Area shifts the area of focus northwestward into San Luis Obispo and Santa Barbara counties while omitting Orange, Riverside, and San Bernardino counties (Figure 2b). This area includes more agricultural and rural areas performing cool season intentional burning as indicated by the consistency of detections during January–May. It also encompasses more warm season fire activity resulting from drier interior regions and elevated terrain, all of which is susceptible during the Mediterranean dry season to human and lightning ignitions. Delayed onset of winter precipitation favors December–January fires such as the 2017 Thomas Fire (uncolored in Figure 2c) and the 2025 Los Angeles Fire Disaster. The Southern California Mountains/Northern Baja Pyrome spans interior Santa Barbara County to San Diego County (Figure 2d) and as a result indicates an extensive wildfire season from May–early January that also includes cool season intentional burning. By including San Diego County fires in October 2003 (green) and 2007 (uncolored), other fire activity appears muted in comparison.

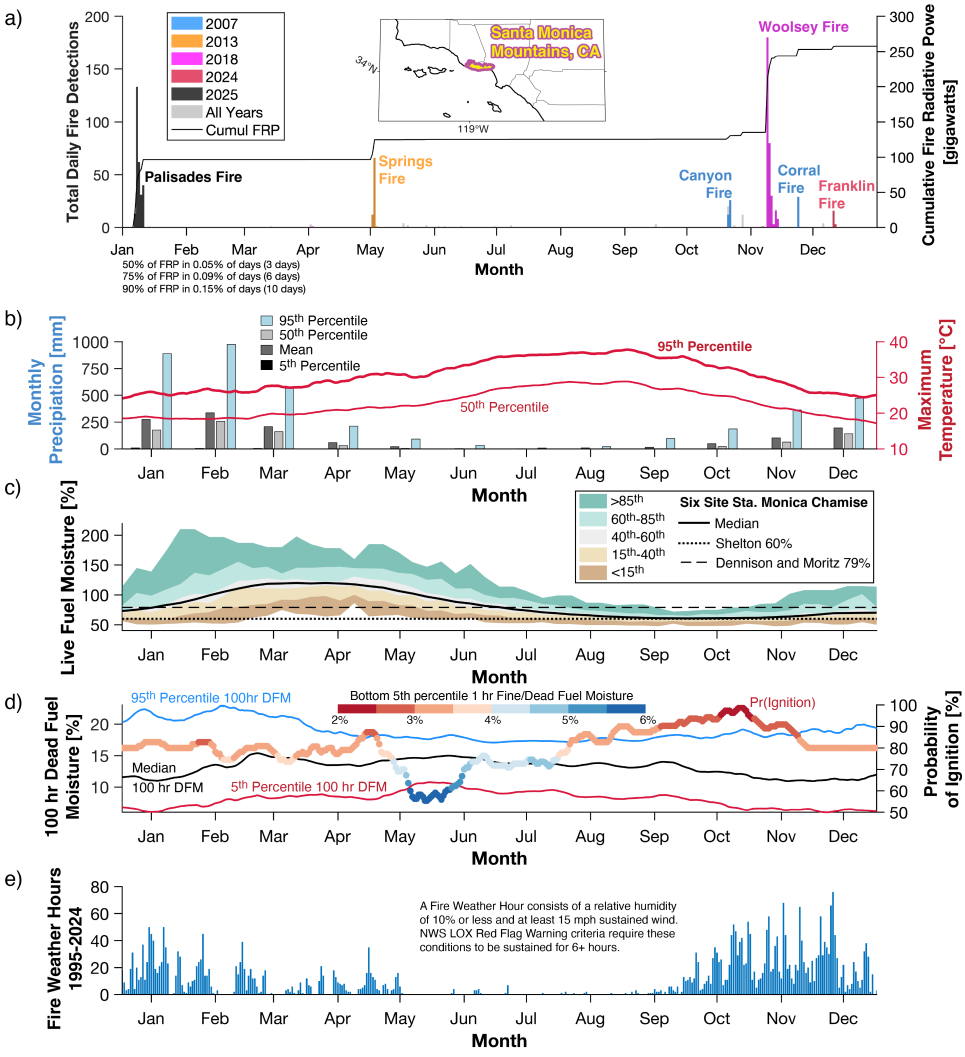

Figure 3: (a) Pyroclimograph showing daily (bars; left y-axis) and cumulative (black line; right y-axis) MODIS-based satellite fire detections for the Santa Monica Mountains of California (inset map) with notable fires named and colored. (b) Monthly mean precipitation distributions (colored bars; left y-axis) and 50^{th} and 95^{th} percentile maximum daily temperature (red lines; right y-axis), both calculated spanning 1979–2025 using gridMET (Abatzoglou, 2013). (c) Measured live fuel moisture for chamise (*Adenostoma fasciculatum*) across six sites. (d) Monthly mean 100-hour dead fuel moisture distributions (colored lines; left y-axis) calculated spanning 1979–2025 using gridMET. Top daily 5^{th} percentile probability of ignition (circles) colored by the lowest 5^{th} percentile one-hour fine and dead fuel moisture (right y-axis); both calculated from lookup tables (National Wildfire Coordinating Group, 2025) at the Malibu Hills Remote Automatic Weather Station (RAWS) for the period spanning January 1995–February 2026. (e) Total daily fire weather hours calculated from the Malibu Hills RAWS using the criteria for the National Weather Service Fire Weather Zones 369 and 370.

4.3. Towards a more complete pyroclimograph

Our motivation to extend the monthly-scale pyroclimograph proposed by Swetnam et al. (2011) centers on the providing a more complete picture of fire activity and the fire environment at daily timescales. The Santa Monica Mountains–spanning coastal Ventura and Los Angeles counties–offer an ideal location to demonstrate how fire weather deviates from climatological conditions. Here, occasional (i.e., 10 days contribute 90% of total FRP), but often-high-impact wildfires can occur throughout the year (Figure 3a).

Monthly precipitation and temperature ranges (Figure 3b) suggest why occasional fires occur despite otherwise a quiescent climate. There is a pronounced seasonal cycle of wet winters, dry summers, and hit-or-miss precipitation during spring and fall on average. Yet every month can be nearly completely dry, increasing fuel receptivity, and winter months can be very wet, contributing to fine fuel growth. While the seasonal cycle of cool temperatures during winter–spring is followed by consistently dry summers and peak warmth in late summer-early fall, the hot end (95^{th} percentile) of cool season daily maximum temperatures can still achieve median summer temperatures. Although live fuel moistures also demonstrate a seasonal cycle driven by plant phenology and resource availability, extended drought can cause these values to remain in the critical range nearly anytime (Figure 3c).

The 100dfm (Figure 3d) represents the characteristic size class of the upper bound of standing dead vegetation in chaparral-dominated ecosystems. The most pronounced seasonal variation of 100dfm occurs from mid-fall to late winter, with a smaller range during the spring-early fall. Values from October to January may approach 5% during drought conditions and exceed 20% during prolonged wet/cool conditions. The median ranges between 11–14% throughout the year. The hot end (i.e., most receptive) of FDFM highlights additional climatological impacts driven by weather phenomenon. While it indicates much of the year can have PIG on 'worst case slopes' in the 70-80% range, it reflects the signal of the spring marine stratus layer in May and June. FDFM also shows two relative maxima of fuelbed receptivity, a subtle peak prior to marine layer onset in April and the signal of the peak October hot and dry season in Southern California with values of 90-100%.

Until now, the pyroclimograph has focused on the ignition component of the fire environment. Inclusion of wind, and particularly wind associated with low relative humidity, incorporates the spread component. Using the weather criteria for Red Flag Warnings but omitting the duration constraint, dry and windy conditions are found to be relatively rare from May-September before

increasing around mid-September and reaching a peak in frequency during October-November (Figure 3e). They decline through the winter before a secondary peak starts in March and peaks in April . Just as the FDFM highlighted the marine stratus season, fire weather hours highlight two critical fire weather patterns affecting the coastal Transverse Ranges: the fall–winter Santa Ana season followed by the spring Sundowner Winds (Hatchett et al., 2018).

5. Discussion

Daily-scale pyroclimographs, made possible by high temporal resolution satellite data, allows a more granular temporal and spatially-explicit perspective than products such as historic fire perimeters that offer only singular dates of discovery and containment (Swetnam et al., 2011) or monthly aggregations of satellite data (Giglio et al., 2009; Sablan et al., 2024). It also allows for agricultural or prescribed burns to be included, assuming burning occurred during satellite overflight, without acquiring burn permit data (Worsnop et al., in revision). However, our approach visualizes a minimum of fire activity: satellites do not capture all pixels burning at all times as wildland fire progresses across the landscape and cannot capture fires that do not produce a detectable heat signature. An upcoming challenge for data continuity will be to merge MODIS and VIIRS detection climatologies as the MODIS mission will be decommissioned by 2027.

Reporting climatological mean conditions likely underestimates the potential for fire activity, which may only require several days or hours to yield favorable conditions for ignition, spread, and extreme fire behavior. It also prevents clear identification of the frequency, timing, magnitude, and duration of anomalous conditions favoring wildland fire, which may or may not be intentional or beneficial (Hatchett and Wells, 2026). Because many fire-prone regions are characterised by variability of environmental conditions on intraseasonal, interseasonal, and interannual timescales, inclusion of fire weather variability, as done here, only provides a first-order glimpse of the potential for fire. Identifying the specific conditions associated with burning will aid the identification of the atmospheric processes driving them, improving their predictability. Subsequent iterations of pyroclimographs will include local conditions extracted on the day of burning to place these into climatological context.

6. Closing Remarks

We revisited the concept of pyroclimographs as simple visualizations leveraging satellite remote sensing to demonstrate a facet of pyrogeography: the "where of fire when" as an aid to understand "the why of fire". Providing a daily perspective of wildland fire activity across decades, pyroclimographs contextualize a region's satellite-era fire history and support the interpretation of past fire events, especially if complemented with additional fire environment data. With no additional information, a pyroclimograph indicates when fire activity has not (yet) been observed, when fire activity may be common but of less intensity (i.e., prescribed and agricultural burning), and when fire activity is most intense (i.e., wildfire season). By including environmental data pertaining to aspects of the fire environment and its variability, a more comprehensive picture emerges of why certain seasons typically do or do not have increased fire activity and why anomalous events occurred. The simplicity of pyroclimographs is intentional; it is our aim that they can be used not just for research purposes but also educational and training purposes for broad audiences to understand the relationship of wildland fire to a place.

7. Code Availability

Matlab code to produce pyroclimographs is available upon request; it is slated to be released publicly in mid-2026.

8. Acknowledgements

I greatly appreciate discussions on improving earlier versions of pyroclimographs with Todd Lindley, Alan Rhoades, and Eli Orland.

References

Abatzoglou, J.T., 2013. Development of gridded surface meteorological data for ecological applications and modelling. International Journal of Climatology 33, 121–131. doi:https://doi.org/10.1002/joc.3413.

Al-Yaari, A., Condom, T., Junquas, C., Rabatel, A., Ramseyer, V., Sicart, J.E., Masiokas, M., Cauvy-Fraunié, S., Dangles, O., 2023. Climate variability and glacier evolution at selected sites across the world: Past trends

and future projections. Earth's Future 11, e2023EF003618. doi:https://doi.org/10.1029/2023EF003618.

Brown, T., Shelton, J., 2025. Confluence of fire and people. Nature Sustainability 8, 329–330. doi:10.1038/s41893-025-01541-9.

California Annual Operating Plan, 2025. California Annual Operating Plan 2025. https://www.weather.gov/media/wrh/cafw/2025_CA_FIRE_AOP.pdf.

Dennison, P.E., Moritz, M.A., 2009. Critical live fuel moisture in chaparral ecosystems: a threshold for fire activity and its relationship to antecedent precipitation. International Journal of Wildland Fire 18, 1021–1027. doi:10.1071/WF08055.

Giglio, L., Loboda, T., Roy, D.P., Quayle, B., Justice, C.O., 2009. An active-fire based burned area mapping algorithm for the modis sensor. Remote Sensing of Environment 113, 408–420. doi:https://doi.org/10.1016/j.rse.2008.10.006.

Guirguis, K., Hatchett, B., Clemesha, R., Aguilera, R., Gershunov, A., Campbell, I., Cayan, D., Merrifield, M., 2025. Compound atmospheric drivers of the catastrophic 2025 los angeles urban firestorm. npj Natural Hazards 2, 103. doi:10.1038/s44304-025-00155-7.

Hatchett, B.J., Smith, C.M., Nauslar, N.J., Kaplan, M.L., 2018. Brief communication: Synoptic-scale differences between sundowner and santa ana wind regimes in the santa ynez mountains, california. Natural Hazards and Earth System Sciences 18, 419–427. doi:10.5194/nhess-18-419-2018.

Hatchett, B.J., Wells, E.M., 2026. Good fire weather. EarthArXiv Preprint doi:https://doi.org/10.31223/X54435.

Lasantha, V., Oki, T., Tokuda, D., 2022. Data-driven versus köppen–geiger systems of climate classification. Advances in Meteorology 2022, 3581299. doi:https://doi.org/10.1155/2022/3581299.

National Wildfire Coordinating Group, 2025. Fire Behavior Field Reference Guide, PMS 437. URL: https://www.nwcg.gov/publications/pms437. Last Accessed: 2026-02-04.

Sablan, O., Ford, B., Gargulinski, E., Hammer, M.S., Henery, G., Kondragunta, S., Martin, R.V., Rosen, Z., Slater, K., van Donkelaar, A., Zhang, H., Soja, A.J., Magzamen, S., Pierce, J.R., Fischer, E.V., 2024. Quantifying prescribed-fire smoke exposure using low-cost sensors and satellites: Springtime burning in eastern kansas. GeoHealth 8, e2023GH000982. doi:https://doi.org/10.1029/2023GH000982.

Senande-Rivera, M., Insua-Costa, D., Miguez-Macho, G., 2022. Spatial and temporal expansion of global wildland fire activity in response to climate change. Nature Communications 13, 1208. doi:10.1038/s41467-022-28835-2.

Short, K.C., Grenfell, I.C., Riley, K.L., Vogler, K.C., 2020. Pyromes of the conterminous united states. Fort Collins, CO: Forest Service Research Data Archive. doi:https://doi.org/10.2737/RDS-2020-0020.

Snethlage, M., Geschke, J., Spehn, E., Ranipeta, A., Yoccoz, N., Körner, C., Jetz, W., Fischer, M., Urbach, D., 2022a. Gmba mountain inventory v2. URL: https://earthenv.org/mountains, doi:10.48601/EARTHENV-T9K2-1407.

Snethlage, M.A., Geschke, J., Ranipeta, A., Jetz, W., Yoccoz, N.G., Körner, C., Spehn, E.M., Fischer, M., Urbach, D., 2022b. A hierarchical inventory of the world's mountains for global comparative mountain science. Scientific Data 9, 149. URL: https://doi.org/10.1038/s41597-022-01256-y, doi:10.1038/s41597-022-01256-y.

Swetnam, T.W., Falk, D.A., Sutherland, E.K., Brown, P.M., Brown, T.J., 2011. Final report, 2011: Fire and climate synthesis (facs) project, jfsp 09-2-01-10. https://www.researchgate.net/publication/292610619_Final_Report_2011_Fire_and_Climate_Synthesis_FACS_Project_JFSP_09-2-01-10.

The MathWorks Inc., 2024. Matlab version: 24.1.0 (r2024a). URL: https://www.mathworks.com.

Worsnop, R.P., Hoell, A., B.J., H., T.B., C., Breeden, M.L., Zach Tolby, Z., Short, K.C., Hobbins, M., in revision. Characterizing windows of opportunity for prescribed pile and broadcast burning in northern california. Fire Ecology .